

Microphysical properties of stratocumulus clouds during ACE-2

By HANNA PAWLOWSKA[†] and JEAN-LOUIS BRENGUIER*, ¹METEO-FRANCE (CNRM/GAME), Centre National de Recherches, 42 av. Coriolis, 31057, Toulouse, Cedex 01, France

(Manuscript received 29 March 1999; in final form 1 October 1999)

ABSTRACT

Microphysical measurements performed during 8 flights of the CLOUDYCOLUMN component of ACE-2, with the Meteo-France Merlin-IV, are analyzed in terms of droplet number concentration and size. The droplet concentration is dependent upon the aerosol properties within the boundary layer. Its mean value over a flight varies from 55 cm^{-3} , for the cleanest conditions, to 244 cm^{-3} , for the most polluted one. For each flight, the variability of the concentration, in selected cloud regions that are not affected by mixing with dry air or drizzle scavenging, ranges from 0.5 to 1.5 of the mean value. The mean volume diameter increases with altitude above cloud base according to the adiabatic cloud model. The frequency distribution of mean droplet volume normalized by the adiabatic value, for the selected regions, shows the same dispersion as the distribution of normalized concentration. The values of droplet concentration versus mean volume diameter are then examined in sub-adiabatic samples to characterize the effects of mixing and drizzle scavenging. Finally, the ratio of mean volume diameter to effective diameter is analyzed and a simple relationship between these 2 crucial parameters is proposed.

1. Introduction

The experimental strategy in CLOUDYCOLUMN was designed for simultaneous measurements of aerosol, cloud microphysical and radiative properties of stratocumulus cloud (see the CLOUDYCOLUMN overview in Brenguier et al. (2000b), hereafter referred to as CCO). Such an approach is particularly suited for a column closure experiment at the scale of a convective cloud cell (1 km). Important results have already been obtained from the comparison of radiative measurements performed from above the cloud layer with radiative properties derived from in-cloud measurements of the microphysics (Brenguier

et al., 2000a). Having validated the process models of interactions between aerosols, cloud microphysics and radiative properties at the scale of a convective cell, the next step towards parameterizations for a GCM is to extrapolate them to the scale of a GCM grid (100 km). The key parameters to consider for the microphysics/radiation interaction are the liquid water content (LWC), the droplet number concentration, and the effective droplet diameter (Brenguier et al., 2000a). These parameters are highly variable in the horizontal and in the vertical. Cloud radiative properties are functions of these parameters integrated over the cloud geometrical thickness, which is also variable. In order to characterize experimentally the interaction between aerosols and cloud radiative properties, despite the variability of the cloud morphology and dynamics, a statistical analysis of cloud microphysics based on a large number of samples is therefore needed.

* Corresponding author.
e-mail: jlb@meteo.fr

[†] On leave from Institute of Geophysics, University of Warsaw, Poland.

CLOUDYCOLUMN provides the largest data set presently available with concomitant measurements of aerosol, microphysical and radiative properties of clouds. The data set is particularly homogeneous in terms of cloud morphology, especially for the cloud geometrical thickness (Fig. 6, CCO). This figure also reveals that the most apparent difference between the various situations is in the droplet concentration, with values of less than 100 cm^{-3} in clean air masses (25 and 26 June), to more than 300 cm^{-3} in the most polluted one (9 July). A preliminary analysis of the microphysical parameters was undertaken. It was found that, within the convective core of the cloud cells, the profiles of these parameters were close to the adiabatic reference, with sub-adiabatic regions between the cells.

The present study has 3 objectives. (1) To identify typical values of the droplet concentration for each situation and to characterize its variability. This especially applies to regions where the droplet concentration is likely to be connected to aerosol properties, i.e., regions that are not affected by mixing with dry air or drizzle scavenging (Section 3). (2) To examine the relationship between the droplet mean volume diameter and the altitude above cloud base, as a function of the droplet concentration (Section 4). The data are analyzed to show how the adiabatic profile observed in unmixed cores is altered by the mixing process and drizzle scavenging, as seen in regions where the number concentration and LWC are significantly reduced. (3) The last objective is to provide information about the relationship between the droplet mean volume diameter and the effective diameter which is used in radiative transfer calculations (Section 5).

The droplet measurements in CLOUDYCOLUMN have been performed with the most accurate airborne droplet spectrometer, the Fast-FSSP (Brennguier et al., 1998). This droplet counter is an improved version of the Forward Scattering Spectrometer Probe (FSSP)* with better size and spatial resolutions. Spatial resolution is as important as size resolution, especially when analyzing frequency distributions of the parameters. The droplet measurements discussed here have been

processed at 10 Hz, i.e., a spatial resolution of about 10 m.

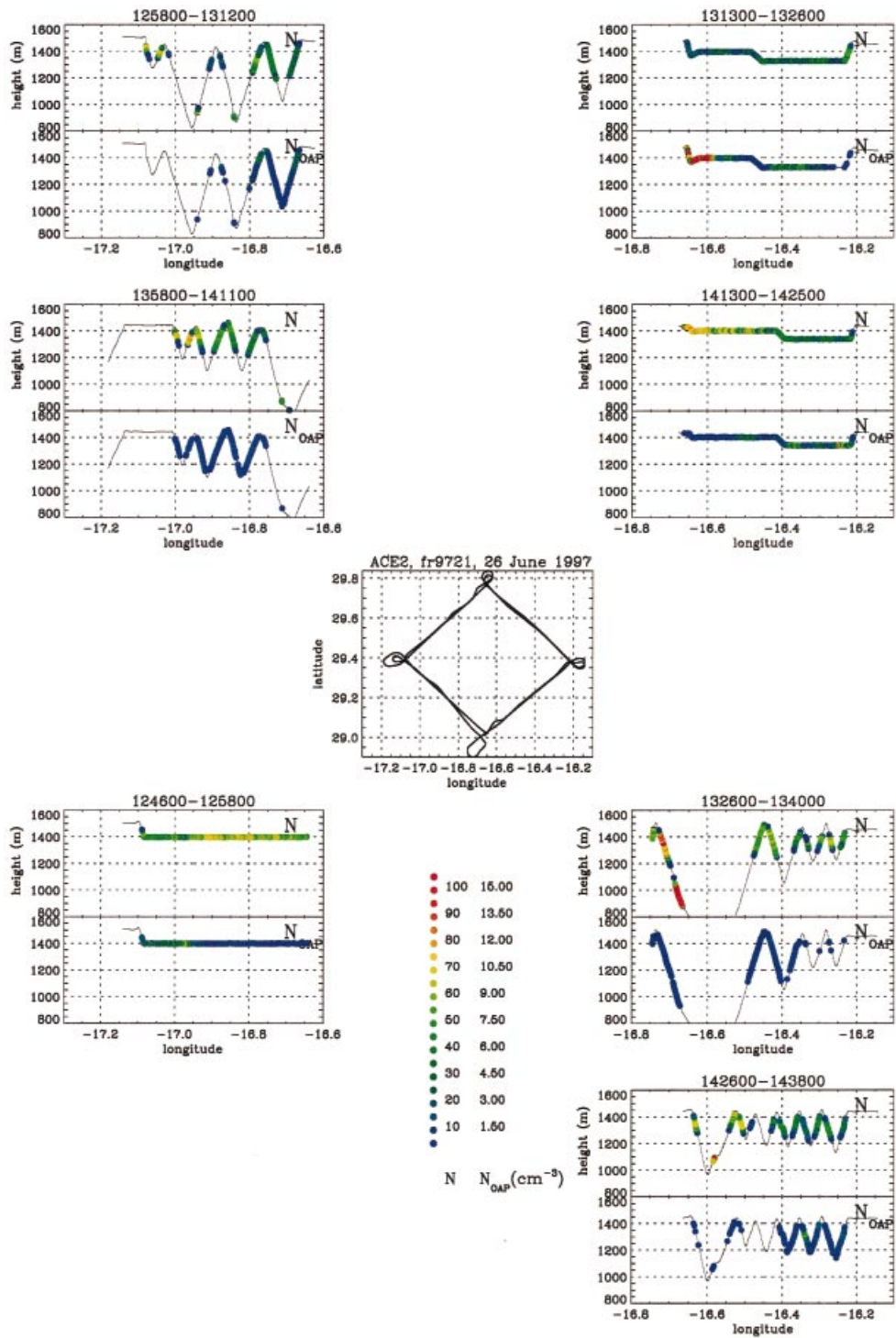
The detection of drizzle particles is based on measurements of particle concentration with a PMS OAP-200X. This instrument covers a size range from 20 to 200 μm diameter. Most of the particles detected during CLOUDYCOLUMN were counted in the first class of the OAP (20–40 μm). The denomination of drizzle for such small particles is slightly incorrect. In fact it is used here as an indication of drizzle formation.

2. Sampling strategy

Various constraints have to be considered when designing a sampling strategy for an instrumented aircraft. A compromise must be found to fulfill different experimental objectives. During ACE-2, the Merlin-IV flight time had to be shared between characterizing the sub-cloud region (turbulent fluxes, aerosols and CCN spectra) and characterizing the cloud layer (cloud microphysics, turbulent fluxes and interstitial aerosol). For measurements of turbulent fluxes and CCN activation spectra, constant level legs are preferable. For microphysical measurements it is necessary to combine 2 different approaches. Constant level legs provide statistics about microphysical parameters at a certain level, however, they are not suited to the characterization of the vertical profiles of microphysics. Vertical sampling is of course impossible with an aircraft, but rapid ascents or descents (5 m/s) still provide a satisfactory description of these profiles. Flight time was thus shared between constant altitude legs, at various levels from below cloud base to cloud top, and series of ascents and descents through the cloud layer.

The selection of the flight track is also a crucial step. The ultimate objective of the experiment is to provide validation data sets for climate models, thus square flight tracks with side lengths of about 60 km were selected. Square flight tracks also allow the remote sensing aircraft (the DLR Do-228), equipped with radiometers and flying 1 km above the cloud layer, to adjust its position during each turn in order to maintain close synchronization with the in situ aircraft. Finally, a closed flight track is well suited for calculations of advection within the domain and provides further initialization of the models. With a flight

* The FSSP is manufactured by Particle Measuring Systems (PMS), Boulder, CO, USA.



duration of about 3.5 h, the Merlin-IV was able to perform almost 3 full squares per flight. Nine scientific flights were flown with square flight tracks. Two additional scientific flights were performed along straight legs in order to document the transition from polluted to marine air masses at larger scales. A summary of the 11 CLOUDYCOLUMN scientific flights is given in CCO.

Fig. 1 illustrates the flight 21 case, on 26 June 1997. The central graph shows the geographical location and square flight track. The graphs on the sides represent the vertical trajectory of the aircraft with droplet N and drizzle N_{OAP} concentrations superimposed on a color scale. The flight starts at 11:56 at the western corner (W), with 3 constant level legs (W–N, N–E, and E–S) below and at cloud base (not shown in the figure). Microphysical measurements start at 12:46 (S–W) with a constant level leg (lower left corner in the figure). The next leg (W–N) lasts from 12:58 to 13:12 with a series of 8 ascents or descents. The flight continues with a N–E constant level leg (1313:1326), a E–S series of ascents and descents (1325:1340), a S–W constant level leg (1343:1354) below cloud base (not shown in the figure), a W–N series of ascents and descents (1358:1411), a N–E constant level leg (1413:1425), and finally a E–S series of ascents and descents (1426:1438). The displayed data clearly illustrate the variability of the microphysical properties within the stratocumulus layer. For example, drizzle formation can be identified within the N–E leg, between 13:13 and 13:25, at the longitude -16.6 (close to the northern corner).

The natural variability of cloud microphysics and dynamics is the most serious drawback in the identification of a relationship between aerosol and microphysical properties at the scale of a cloud system. When flying through a cloud layer, the chances of crossing regions affected by either mixing with dry air or drizzle precipitation are significant. Therefore the analysis of only a few vertical profiles does not lead to statistically significant results. The analysis presented here for 8

flights of the CLOUDYCOLUMN experiment is based on at least 15 cloud profiles per flight (8 and 17 July) and up to 35 profiles on 26 June. The flight on 7 July, which corresponds to the most polluted air mass, is not presented here because the limited number of profiles prevents a statistically significant analysis of the cloud microphysical properties.

3. Characterization of the droplet number concentration

3.1. Scientific background

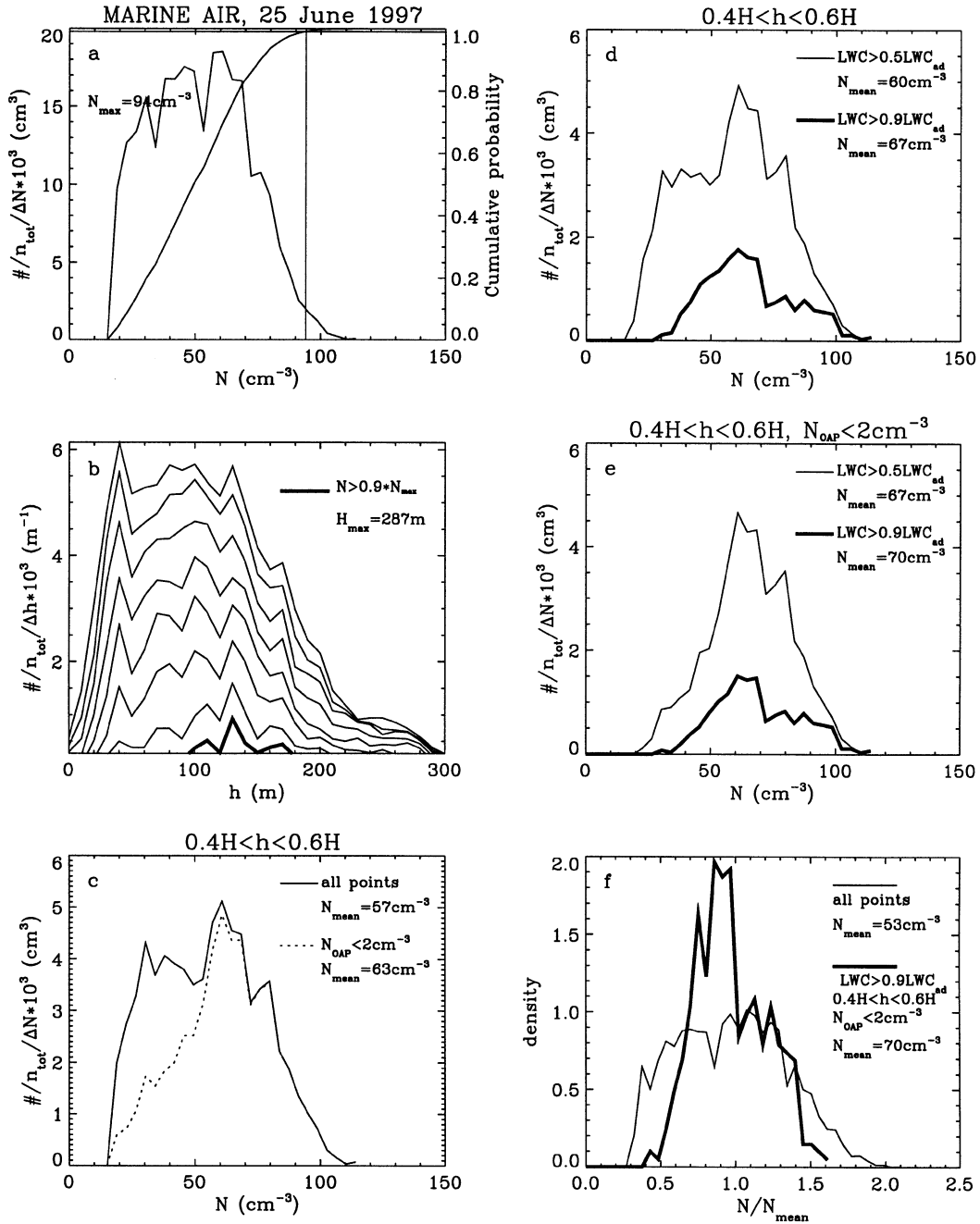
CLOUDYCOLUMN is devoted to the experimental study of the aerosol indirect effect, that is to changes in cloud radiative properties due to changes in aerosol properties. The link between aerosols and radiation starts with the relationship between aerosol properties and the droplet number concentration. For fixed values of the updraft and aerosol properties, the droplet number concentration can be calculated with an activation model (Snider and Brenguier, 2000, hereafter referred to as SB). In general, a polluted air mass contains a larger concentration of aerosol particles than a marine air mass and thus produces a larger droplet concentration.

The variability of the updraft intensity at cloud base is a significant source of variability in droplet number concentration. For a fixed distribution of cloud condensation nuclei, a stronger updraft generally results in a larger droplet concentration. A complete characterization of the nucleating properties of aerosols should include a quantitative assessment of this dependence of droplet concentration on updraft velocity. The main difficulty in the experimental study of this process is that the relationship between aerosols and droplet concentration is only valid within a non precipitating updraft. The values of droplet concentration measured in other regions of the cloud are altered by additional processes such as mixing with the overlying dry air and scavenging of condensation droplets by drizzle.

Fig. 1. Quick-look plots for flight 21, on 26 June. The central graph shows the aircraft track, flown clockwise. The graphs on the sides represent the aircraft altitude versus longitude for legs flown in cloud: lower-left for the S–W leg, upper-left for the 2 E–N legs, upper-right for the 2 N–E legs, and lower-right for the 2 E–S legs. The colors refer to droplet number concentration, N , in the top panel and to the drizzle number concentration, N_{OAP} , in the bottom panel, with color scales as indicated in the figure. Legs flown below cloud base are not shown in the figure.

Our objective in this section is to characterize each situation with a distribution of droplet concentration values that can be further used for the analysis of the aerosol/microphysics interaction.

The following section thus describes the procedure that has been applied for the selection of samples where the droplet concentration is not altered by additional processes or artifacts.



3.2. Observations

The characterization of the droplet number concentration is based on the series of ascents and descents through the cloud layer. These have a better statistical significance than constant level legs for the description of the whole cloud layer. Figs. 2, 3 illustrate the various steps in the selection of appropriate cloud regions, as defined above, for the 25 June case (Fig. 2) and the 9 July case (Fig. 3). Panel (a) is the frequency distribution of the values of droplet number concentration measured over the whole flight during ascents and descents (10 Hz values or about 10 m spatial resolution). The distributions are characterized by a pronounced mode, with frequencies dropping rapidly towards large values, while a plateau is generally observed towards the small values. The origin of such a plateau is not clear, since low values of the droplet concentration can be due either to mixing with dry air or scavenging by drizzle particles. Underestimation of the concentration also occurs when a significant fraction of the droplets exist at sizes smaller than the minimum size detectable by the instrument (2.6 μm for the Fast-FSSP). The concentration value at 99% of the cumulative distribution characterizes the maximum concentration over the flight, N_{max} .

Panel (b) represents the frequency distribution of the measured altitude above cloud base (h), for 10 Hz samples with concentrations larger than pN_{max} (p from 20 to 90%). This figure reveals that most of the large values of concentration are observed in the central section of the cloud. At low altitude, close to cloud base, droplets are small and a significant part of the distribution is below the Fast-FSSP detection threshold. This is particularly noticeable on 9 July which is the most polluted case, with the largest values of droplet concentration and therefore the smallest droplet sizes. Some of the low values on 25 June are also

associated with drizzle. At higher altitudes, close to cloud top, the low values are due to mixing of the cloudy air with the overlying dry air. The value of altitude at 97% of the cumulative distribution, for $N > 0.2N_{\text{max}}$ defines the maximum cloud geometrical thickness H_{max} (hereafter referred to as H).

Panel (c) is similar to (a) for only samples located within a range of altitude between $0.4H$ and $0.6H$ (solid line). As anticipated the distributions get narrower, except for the flights on 25 June and 16 July (not shown), where the proportion of small values of the concentration remains significant. The next step (dotted line in (c)) is to reject samples with values of drizzle concentration greater than 2 cm^{-3} . This threshold value was selected arbitrarily, but was found to characterize well the regions with and without significant amount of drizzle. Since drizzle measurements are available only at 1 Hz, the rejection criterion is applied to the 10 high resolution values of droplet concentration corresponding to the 1 Hz drizzle sample. For the 25 June case the difference between the 2 distributions is noticeable. In fact, 25 June is the cleanest case, with the lowest values of droplet concentration, so that drizzle concentrations are the largest observed during the CLOUDYCOLUMN campaign. The rejection of samples with drizzle, thus reduces significantly the proportion of samples with a low droplet concentration. For the 9 July case, the droplet concentration is large, drizzle production is inefficient, and the drizzle criterion does not narrow the concentration distribution (Fig. 3c, dotted line is overplotted by the solid line).

The last step aims at the rejection of samples affected by mixing. The criterion is based on the comparison between the LWC in the measured sample and the adiabatic value, LWC_{ad} , at the altitude level of the sample. The adiabatic liquid

Fig. 2. Characterization of the droplet number concentration for flight 20, on 25 June. (a) Frequency distribution of the values measured over all ascents and descents through the cloud layer, and the corresponding cumulative distribution with the 99% value, N_{max} indicated by a vertical bar. (b) Frequency distributions of sample altitudes, for samples with a concentration larger than pN_{max} , with p from 0.2 to 0.9. The value of altitude at 97% of the cumulative distribution for $N > 0.2N_{\text{max}}$ defines the maximum cloud geometrical thickness H_{max} (hereafter referred to as H). (c) Frequency distribution of the measured concentration, with $0.4H < h < 0.6H$ (solid line), and also drizzle concentration lower than 2 cm^{-3} (dashed line). (d) As in (c) for altitude selection, and $\text{LWC} > 0.5\text{LWC}_{\text{ad}}$ (thin line) or $\text{LWC} > 0.9\text{LWC}_{\text{ad}}$ (thick line). (e) Same as (d) with drizzle selection as in (c). (f) Frequency distribution of measured concentration after drizzle and adiabaticity selection, normalized by N_{mean} . N_{mean} is calculated from the distribution shown in (e) with $\text{LWC} > 0.9\text{LWC}_{\text{ad}}$ (thick line). The thin line corresponds to the whole data set, without selection.

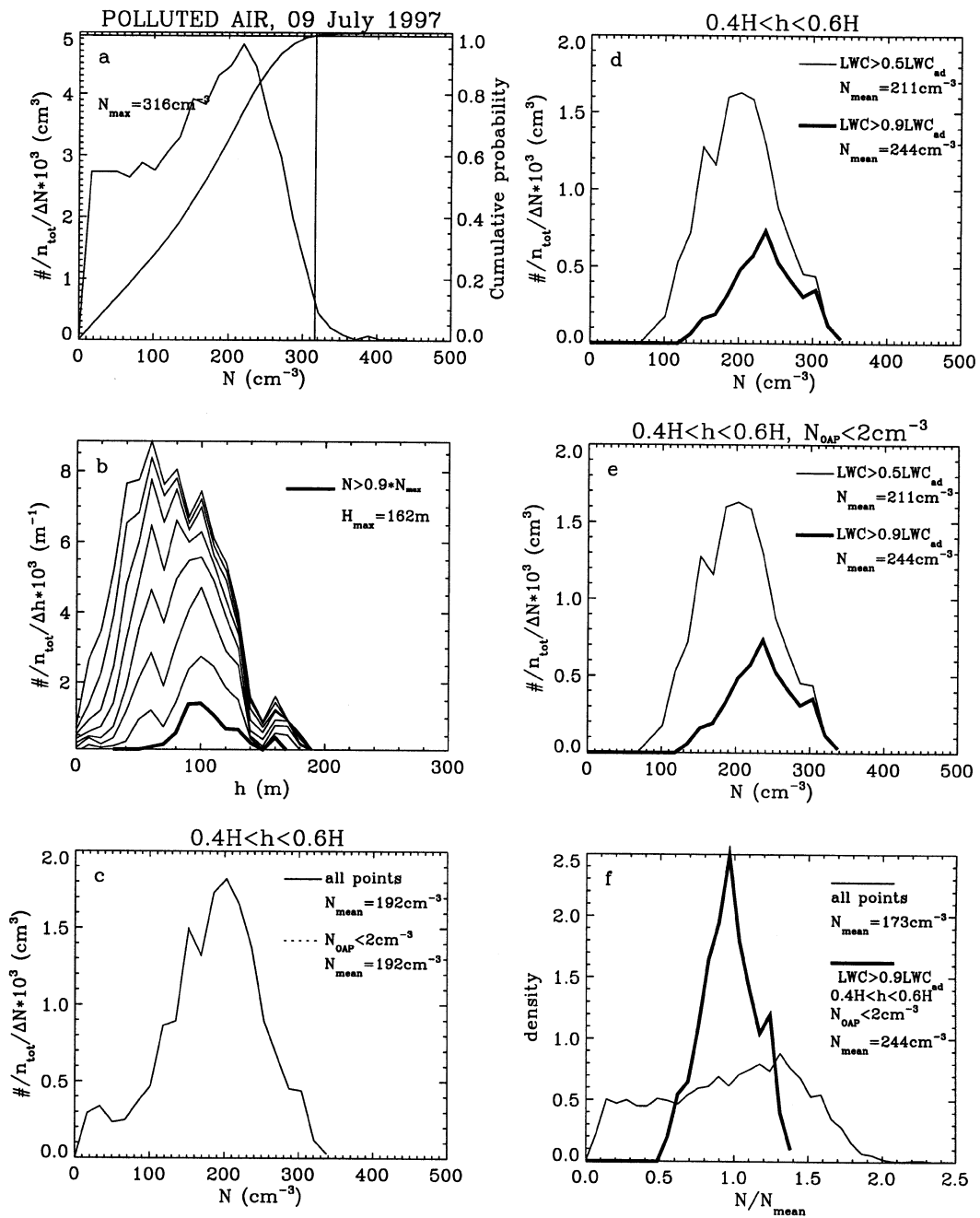


Fig. 3. Same as Fig. 2 for flight 30, on 9 July.

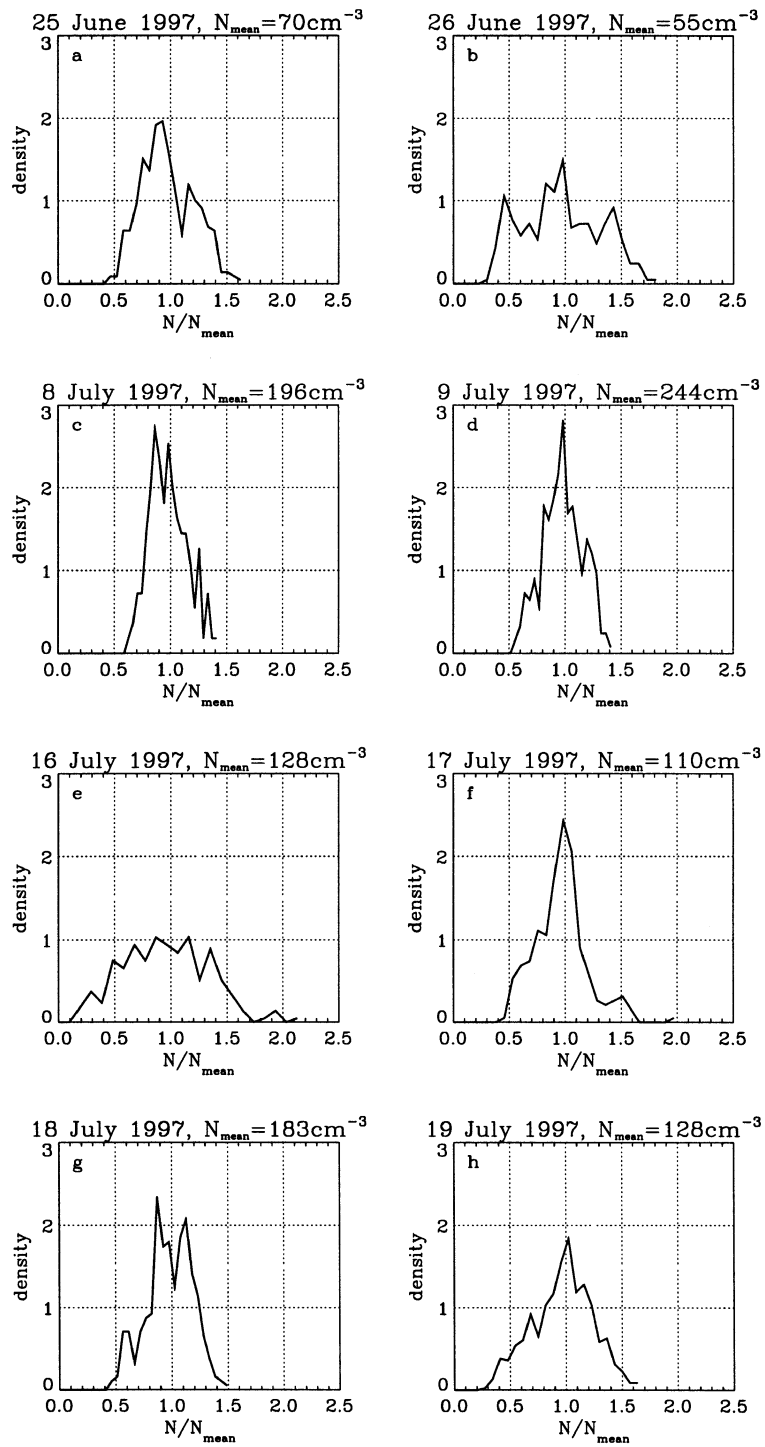
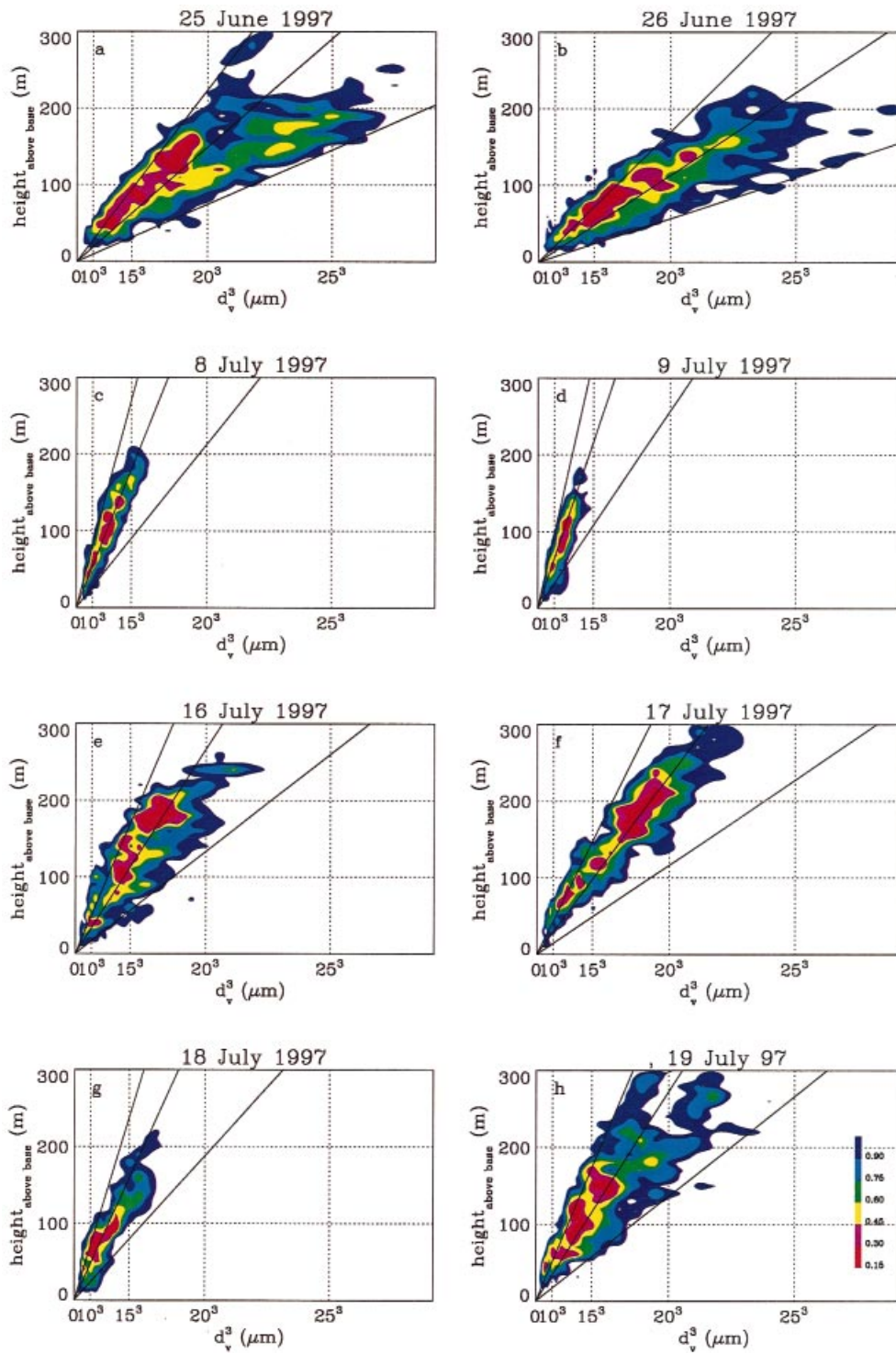


Fig. 4. Same as the thick line in Figs. 2f and 3f for 8 flights of the CLOUDYCOLUMN campaign.



water content at the altitude h above cloud base is calculated as $LWC_{ad} = C_w \cdot h$, where C_w is the moist adiabatic condensate coefficient which is constant over a short altitude range such as through stratocumulus clouds and depends slightly on the temperature in the cloud layer (Brenquier, 1991). Such a criterion of rejection of samples affected by mixing is applied upon the remaining samples after altitude selection, panel (d) and also drizzle selection, panel (e). The frequency distributions of droplet number concentration corresponding to $LWC > 0.5LWC_{ad}$ (thin line) and $LWC > 0.9LWC_{ad}$ (thick line) are plotted. For the 25 June case, N_{mean} increases from 57 (with altitude selection only) to 70 cm^{-3} (with altitude, drizzle selection, and $LWC > 0.9LWC_{ad}$). The proportion of low values has been slightly reduced. The effect of the LWC criterion is more noticeable in the 9 July case; N_{mean} raises from 192 to 244 cm^{-3} (entirely due to the LWC criterion). The mean value of the concentration N_{mean} , calculated from the distribution in (e), with $LWC > 0.9LWC_{ad}$, is selected as a reference for each case.

The last panel (f) shows the frequency distribution of the normalized concentration N/N_{mean} . The thick line corresponds to the distribution after complete selection (altitude, drizzle and LWC), as in (e), while the thin line corresponds to the data set without rejection, as in (a). It must be noted that all the frequency distributions from (a) to (e) have been calculated with respect to the total number of samples in order to show the proportion of samples lost after each selection criterion. However the normalized distribution in (f) after selection (thick line) is calculated with respect to the number of remaining samples in order to emphasize the shape of the distribution. The distribution after selection is narrower than the original distribution (thin line). This demonstrates that, with a large number of vertical profiles, some of the variability in the droplet concentration resulting from mixing with dry air and drizzle scavenging can be removed.

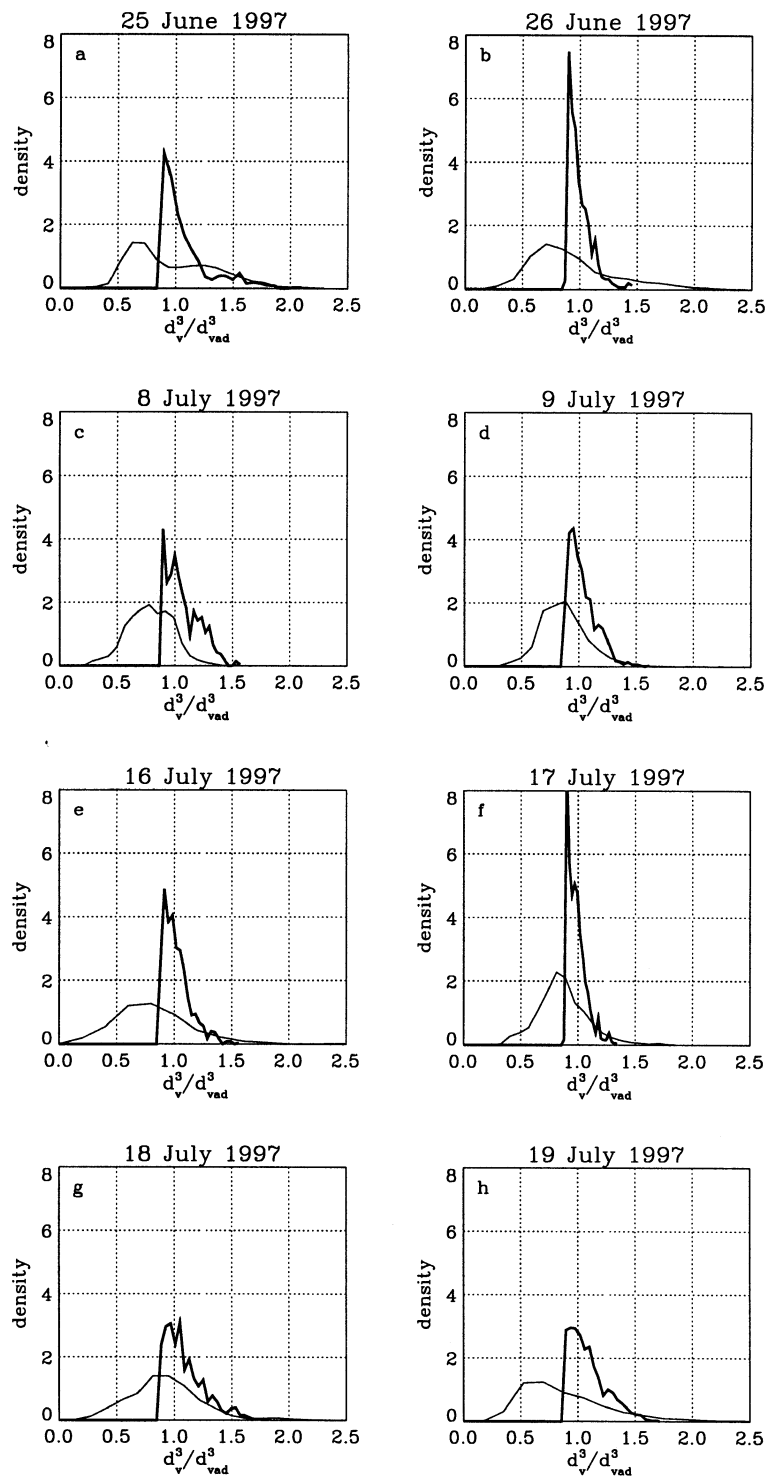
This procedure has been applied to 8 of the scientific flights. The resulting distributions of the

normalized droplet number concentration (similar to the thick line in 2f and 3f) are summarized in Fig. 4. In general the droplet concentration varies between 0.5 and 1.5 of the mean value. The values of mean concentration are particularly small on the 25 June (70 cm^{-3}) and 26 (55 cm^{-3}) cases. These 2 cases will be further considered as a reference for marine aerosol. The largest value is for the flight on 9 July, with a mean of 244 cm^{-3} and a maximum of 316 cm^{-3} (Fig. 3a). The other cases are affected to varying degrees by anthropogenic aerosols, with mean values of the concentration between 100 cm^{-3} and 200 cm^{-3} .

Table 1 compares the mean values of droplet concentration with some preliminary results of the analysis of aerosols properties, such as the condensation nuclei concentration (CN) from measurements at the Hildago station (Rita Van-Dingenen, personal communication), the 2 parameters of the CCN activation spectrum C and k , and the CCN concentration at 0.5% supersaturation measured on board the M-IV (SB). In Table 1, the flights have been ranked based on the N_{mean} values. The 2 extreme cases, 26 June for the marine reference and 9 July for the polluted one, show respectively the smallest and largest values of CCN concentration at 0.5% supersaturation. However, overall, the aerosol properties do not entirely agree with the droplet number concentration classification. For example, the 16 and 19 July cases show very different CN concentrations, while the values of mean droplet concentration are similar. Further analysis is thus needed for a column closure experiment on the activation process. In particular measurements of aerosol and chemical properties performed on board the C130 and the Pelican (Russell and Heintzenberg, 2000; Johnson et al., 2000) might be helpful. The work of SB shows that consideration of both the CCN and the vertical velocity can explain much of the flight-to-flight variability in droplet concentration.

This analysis of the concentration distributions reveals that a cloud system cannot be characterized by a single value of the droplet concentration. The variability in the droplet concentration during a particular flight does not result from a variability

Fig. 5. Isocontours of the mean volume diameter d_v versus altitude of the sample above cloud base h , for the same flights as in Fig. 4. The 3 solid lines correspond to the adiabatic model for N_{ad} equal respectively to $0.5N_{mean}$, N_{mean} , and $1.5N_{mean}$. The colour scale in (h) indicates the fraction of samples within each isocontour.



in the aerosol properties, since aerosols are well mixed horizontally in the boundary layer as indicated by CCN measurements performed below cloud base (SB). It is rather due to the variability of the updraft intensity at the cloud base. Additional processes such as mixing with the overlying dry air and scavenging by drizzle particles also contribute to the variability. Finally, instrumental artifacts are likely to affect the measurements when the droplet sizes are close to the limits of the instrument range. The 2 examples presented demonstrate that the procedure of rejection of samples where the values of droplet concentration have been altered by either mixing with dry air, drizzle or instrumental artifact is effective at reducing the observed variability. Nevertheless, the resulting distributions are still broad with values ranging from 0.5 to 1.5 times the mean value of the droplet concentration. Despite this natural variability, the difference between marine air masses and the polluted ones is clearly reflected in the mean values of droplet number concentration.

4. Characterization of the droplet sizes

4.1. Scientific background

It has been shown in Section 3 that the cloud droplet number concentration is dependent upon the aerosol properties. However, cloud radiative properties are also dependent upon droplet sizes. More precisely, they are governed by 3 parameters: the extinction coefficient, the single scattering albedo and the asymmetry factor. These parameters characterize the local optical properties and are controlled by the droplet spectrum. They can be parameterized as functions of LWC and droplet effective diameter $d_e = d_v^3/d_s^2$, where d_v is the mean volume diameter and d_s is the mean surface diameter of the droplet size distribution (Hansen and Travis, 1974; Slingo and Schrecker, 1982; Twomey and Cocks, 1989). These parameters are highly variable both in the horizontal and in the vertical, as are the LWC and the droplet

spectra. Cloud radiative properties, reflectivity, absorption and transmissivity, are strongly dependent upon the values of these parameters and their spatial distributions. Simple radiative transfer calculations have been performed with the plane-parallel hypothesis (cloud microphysical properties uniform in the horizontal and in the vertical) (Slingo, 1989). However, cloud inhomogeneities and their effects on cloud radiative properties must be taken into account for more accurate predictions of the aerosol indirect effect (Cahalan et al., 1995; Barker, 1996).

The most obvious discrepancy between an idealized plane-parallel model and actual clouds is the vertical profile of the droplet size distribution. The LWC in an adiabatic convective parcel increases almost linearly with altitude, $LWC_{ad}(h) = C_w h$ (Brenquier, 1991). Since the droplet concentration is constant in an adiabatic parcel, the mean droplet volume also increases linearly with altitude:

$$d_{vad}^3 = \frac{C_w h}{\frac{1}{6}\pi\rho_w N_{ad}}. \quad (1)$$

The variability of the actual droplet spectra with respect to the adiabatic reference arises from the same processes that control the variability of the droplet number concentration (mixing and drizzle). The adiabatic reference corresponds to a convective parcel which originates from the cloud base and ascends without mixing with the environmental air. As long as the droplet number concentration is constant (adiabaticity), the process is reversible during up- and downward motions of the parcel. The droplet concentration, however, can be affected in stratocumulus clouds by cycling circulations of the cloud parcels through the layer. In such a case, the process is no longer reversible and the droplet concentration can be progressively reduced by deactivation of some nuclei (Korolev, 1995).

When the parcel is mixed with dry air, the number concentration is reduced by dilution and evaporation of some droplets. The mixing process can be either homogeneous or inhomogeneous (Baker et al., 1980). During a homogeneous process, all the droplets are exposed to the same

Fig. 6. Distributions of mean volume diameter normalized by the adiabatic value d_v/d_{vad} , for the same 8 flights as in Fig. 4. Thin line: samples with $h > 0.4H$ and d_{vad} calculated with $N_{ad} = N_{mean}$. Thick line: samples with $h > 0.4H$, $N_{OAP} < 2 \text{ cm}^{-3}$, $LWC > 0.9LWC_{ad}$, and d_{vad} calculated with $N_{ad} = N_{sample}$, where N_{sample} is the droplet concentration actually measured in the sample.

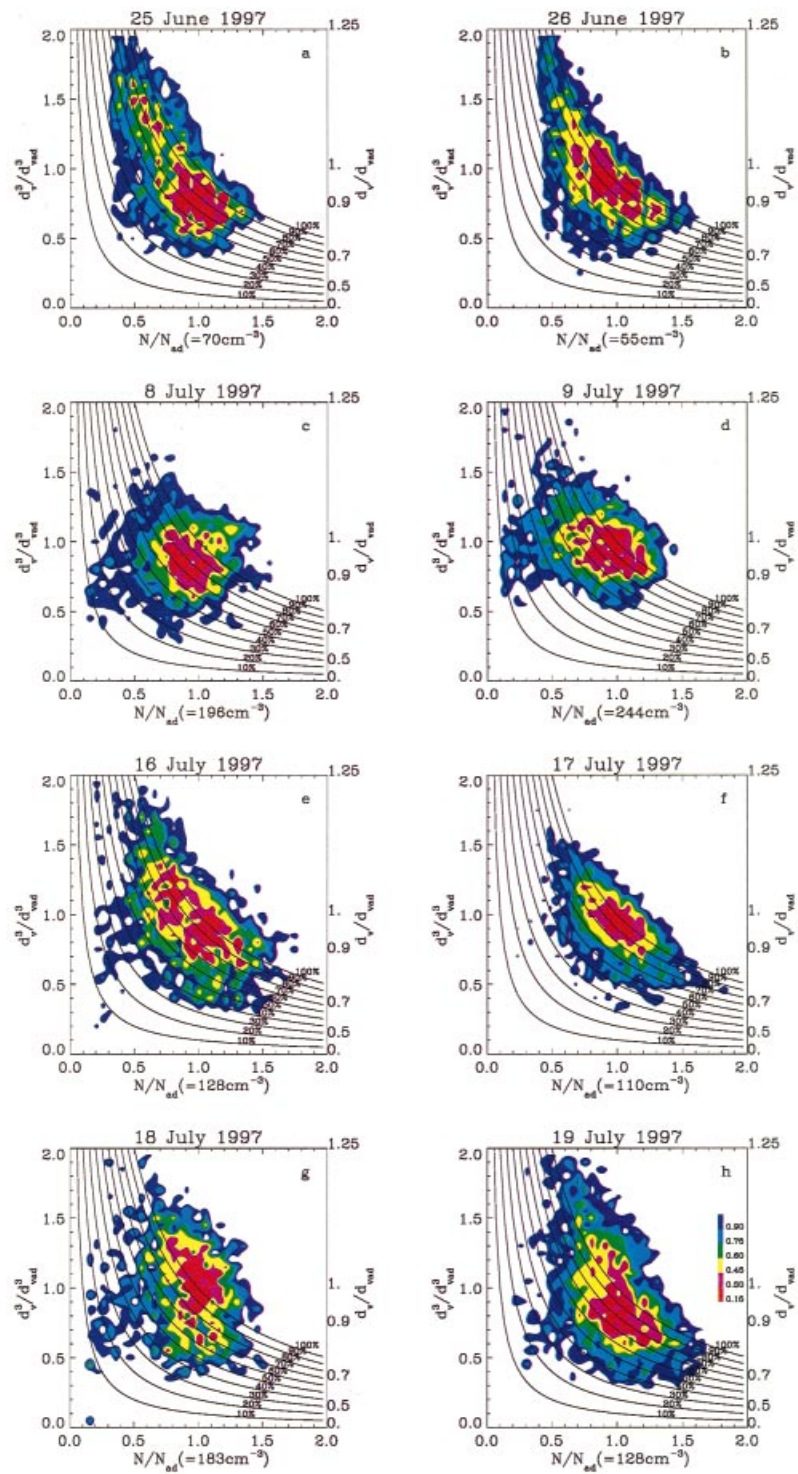


Table 1. Summary of the 8 flights, with date, mean droplet concentration, N_{mean} , condensation nuclei concentration, CN, the C and k coefficients of the CCN activation spectra, and the concentration of activated CCN at 0.5% supersaturation

Date	N_{mean}	CN	CCN C	CCN k	CCN 0.5%
26 June	55	320	125	1.02	62
25 June	70	360	132	0.4	100
17 July	110	580	550	0.90	295
16 July	128	590			
19 July	128	1030	340	0.55	232
18 July	183	1090	750	1.13	343
8 July	196	3090			
9 July	244	1170	520	0.44	383

subsaturation and partially evaporated until the mixed parcel reaches saturation. The reduction in droplet concentration is concomitant with a reduction in droplet sizes. During an inhomogeneous mixing process, some regions of the parcel are fully evaporated until the entrained air comes to saturation. The remaining droplets are not affected by evaporation. In such a case the droplet number concentration is more reduced than during a homogeneous process (by dilution and by total evaporation of some droplets). However the shape of the droplet spectrum is not modified, so that the mean volume diameter is constant. The transition from homogeneous to inhomogeneous mixing is determined by the evaporation time scale which is proportional to the droplet surface. The 9 July case shows a mean droplet diameter 2 times smaller than the 25 June case, that is droplet surfaces 4 times smaller. This change in droplet size could explain the different responses to the LWC criterion discussed in Subsection 3.2.

After the concentration has been reduced by mixing, further ascent or descent of the parcel will result in some deviation from the adiabatic reference, according to $\Delta d_v^3 = C_w \Delta h / (\frac{1}{6} \pi \rho_w N)$, where $N < N_{\text{ad}}$. The changes in droplet size with altitude are thus more important than in an adiabatic parcel, with a faster evaporation during a descent and a faster growth during ascent. If the total droplet surface has been significantly reduced,

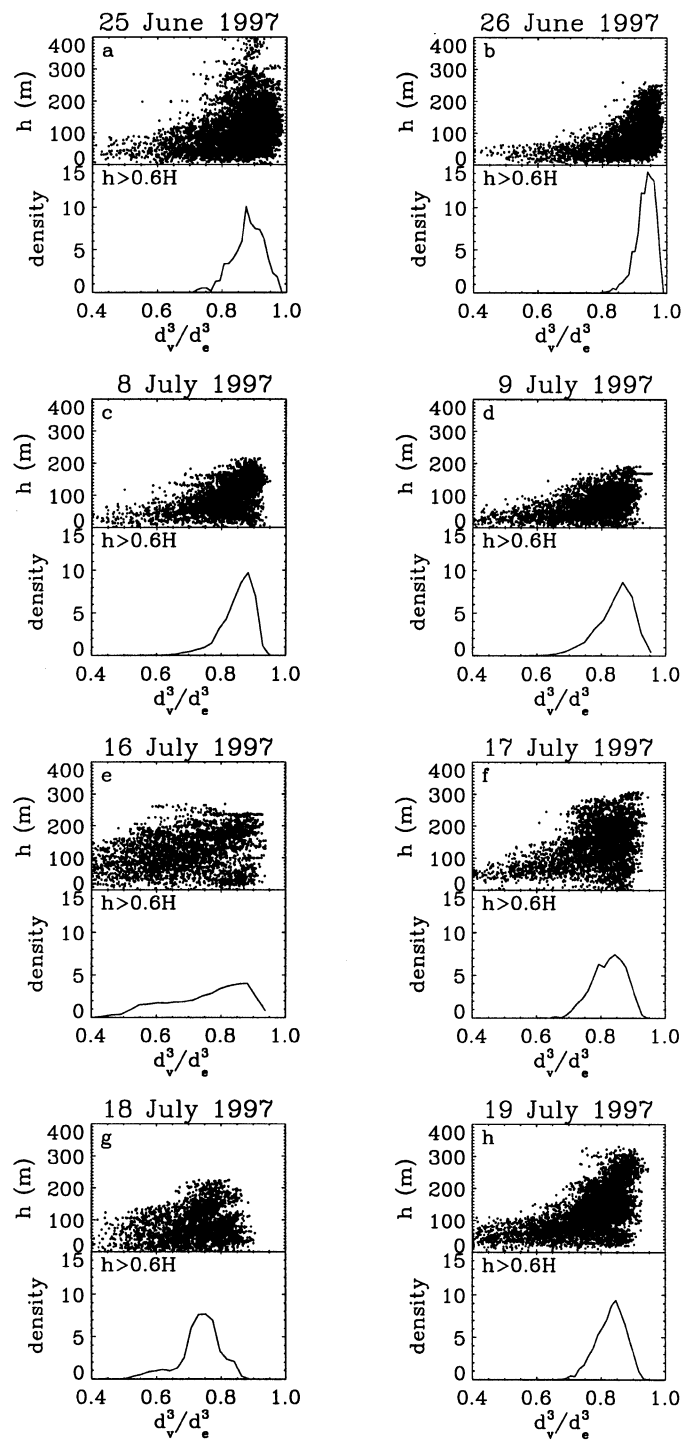
there is a possibility of activation of new nuclei, with the appearance of very small droplets in the spectrum. Finally, mixing between parcels of different origins and kinematics, as well as scavenging by drizzle, produce broad spectra. The analysis of the measurements aims at the identification of the most significant processes and the characterization of the resulting spectra.

4.2. Vertical profile of mean volume diameter

As was done for the characterization of the droplet number concentration, the series of ascents and descents were used here rather than the horizontal legs to better document the whole cloud layer. Fig. 5 shows the isocontours of frequency distribution of mean volume diameter d_v versus altitude above cloud base, h , for the 8 flights already presented in Fig. 4, without any selection criterion. The 3 solid lines in each graph correspond to the linear relationship between d_{vad}^3 and h as predicted by eq. (1), with values of N_{ad} respectively equal to $0.5N_{\text{mean}}$, N_{mean} , and $1.5N_{\text{mean}}$. The values of N_{mean} for each flight are the same as in Fig. 4. This summary of the campaign reveals that droplet sizes are increasing with altitude, as predicted by the adiabatic model, with a variability corresponding to the observed variability in droplet concentration. The difference between the flights, in terms of microphysical properties, is enhanced when considering the vertical profile of droplet diameters, compared to droplet number concentration: 9 July thus appears as the most polluted flight, followed by 8 and 18 July; 16, 17, and 19 July show properties intermediate between marine conditions and the polluted ones, while 25 and 26 June exhibit pure marine characteristics. In particular, it is noted that the precipitation efficiency is likely to be higher for the 25 and 26 June flights, with values of d_v larger than 25 μm , while it is probably very low for the 9 July case, with values of d_v smaller than 15 μm . This specific question will be addressed in a forthcoming paper.

As was done for the droplet number concentration, the mean volume diameter d_v has been

Fig. 7. Isocontours of the measured concentration normalized by N_{mean} , versus d_v^3 normalized by d_{vad}^3 , for the same flights as in Fig. 4. The solid lines indicate LWC values from 10% to 100% of LWC_{ad} . Right-hand axis gives values of d_v/d_{vad} . The colour scale in (h) indicates the fraction of samples within each isocontour.



normalized. The adiabatic LWC is calculated for each sample from its altitude above cloud base. The value is then divided by N_{mean} to derive the adiabatic mean volume diameter d_{vad} . The distribution of $(d_v/d_{\text{vad}})^3$ is plotted in Fig. 6 for the 8 flights. The cube of the diameter ratio is used for a better comparison with the concentration variability, since $\text{LWC} \propto Nd_v^3$. The thin line represents the frequency distribution of the ratio, for samples higher than $0.4H$. The value of d_{vad} is derived from (1) with $N_{\text{ad}} = N_{\text{mean}}$. Droplet spectra measured at a lower altitude are rejected because they are truncated by the instrument and because the low values of d_{vad} are affected by errors in the estimation of the cloud base altitude. The peak of the distribution is located between 0.7 and 0.9, that is mean volume diameters between 89% and 96% of the adiabatic value. The distribution extends from about 0.2 (16 July) to 2 (19 July), that is a dispersion slightly larger than the dispersion of the concentration distributions. The thick line corresponds to the frequency distribution of the $(d_v/d_{\text{vad}})^3$ ratio at altitudes higher than $0.4H$ and the same LWC and drizzle selection criteria as for the concentration ($\text{LWC} > 0.9\text{LWC}_{\text{ad}}$ and $N_{\text{OAP}} < 2 \text{ cm}^{-3}$). The adiabatic reference is now derived from (1) with $N_{\text{ad}} = N_{\text{sample}}$, where N_{sample} is the droplet concentration actually measured within the sample. The dispersion is significantly reduced, with the largest frequency at values slightly lower than the adiabatic. The maximum values of the ratio are smaller than 1.5 of the adiabatic reference. In Fig. 6, the difference between the 2 distributions is mainly due to the value selected for N_{ad} , either N_{mean} or N_{sample} . In fact, the selection of the samples with respect to adiabaticity or the absence of drizzle does not improve significantly the variability in droplet size. This feature suggests that most of the size variability is related to fluctuations of the droplet concentration and that cloud cells, with a certain droplet concentration at the CCN activation level, keep their identity during their ascent through the cloud layer. This statement will be further validated in the next section. Fig. 6 demonstrates that the adiabatic model provides an accurate description

of droplet growth in stratocumulus despite the effects of mixing and drizzle scavenging.

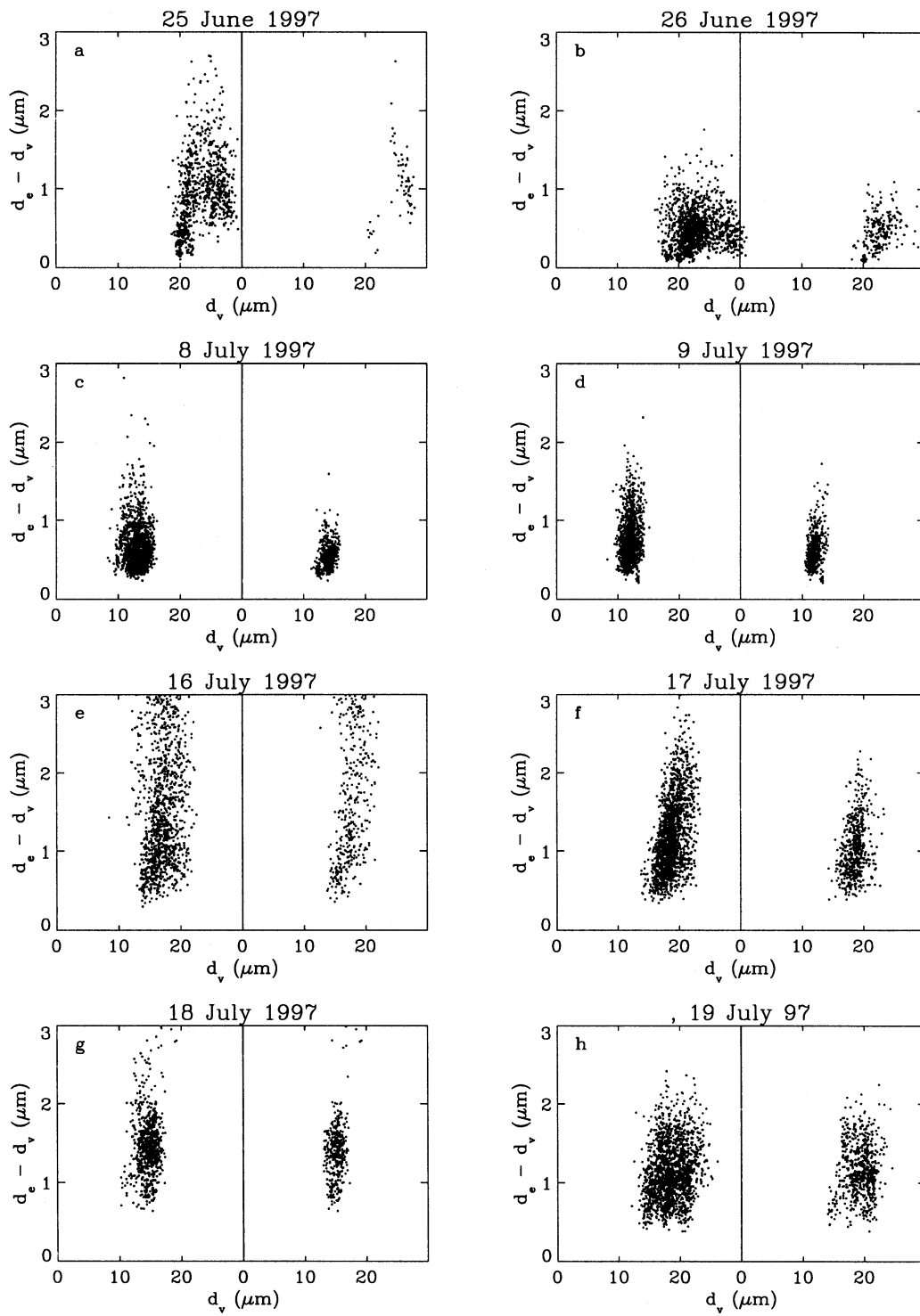
4.3. Concentration/size correlation

Fig. 6 suggests that the concentration of CCN activated at the base of the convective cores determines the spectral shape up to the cloud top and that the 2 processes which affect droplet number concentration, namely mixing with dry air and drizzle scavenging, do not further modify significantly the spectral shape. For drizzle scavenging, this observation can be explained by the fact that collection efficiency depends on the fall velocity difference between a collecting drop and the collected droplets. As a first approximation, it can be assumed that cloud droplets are so small, that their fall velocity is negligible. Thus, all the droplets in a spectrum have the same probability of being collected by a drop, entirely determined by the collecting drop size. Therefore drizzle formation shall not affect the original droplet size distribution. In order to understand the effect of mixing it is valuable to consider concurrently the values of droplet number concentration and diameter in each sample (10 Hz). Fig. 7 summarizes this analysis. The X axis is the droplet number concentration normalized by its mean value. The adiabatic LWC is then calculated from the altitude h of the sample and the measured value of mean volume diameter is normalized by the adiabatic value, d_{vad} , derived from eq. (1) with $N_{\text{ad}} = N_{\text{mean}}$. The point with coordinates (1, 1) thus corresponds to an adiabatic LWC value. All points along the 100% isoline ($X \times Y = 1$) represent samples with values of concentration and sizes different from the mean, but with a LWC still equal to the adiabatic value. Other isolines correspond to values of LWC lower than the adiabatic from 90% to 10% of the adiabatic.

There are 2 interesting features to consider in these plots.

(i) Quasi-adiabatic samples: a large proportion of the samples are aligned along the 100% isoline (25 and 26 June, 16, 17 and 19 July). This corresponds to the relation expressed by eq. (1) for

Fig. 8. Distributions of the coefficient $k = d_v^3/d_c^3$ for the same flights as in Fig. 4. Upper panel: scatter plot of the k values versus sample altitude above cloud base (h). Lower panel: frequency distribution of k for samples above $0.6H$.



regions that are not affected by mixing or drizzle. Typically, regions of concentration lower than the average are characterized by larger droplets. This feature implies that such regions are ascending from the cloud base with a constant value of the droplet concentration, and that the variability of droplet concentration arises from fluctuations of the updraft speed at the cloud base.

(ii) Sub-adiabatic samples: sub-adiabatic values of LWC are principally due to a reduction of the concentration rather than a reduction of the droplet size. For example, on 8 and 9 July, values as low as 10% of LWC_{ad} have been observed, with concentration values of the order of $0.1N_{mean}$, while d_v^3 is never lower than 0.6 of its reference value. This feature is referred to in the literature as inhomogeneous mixing. The same feature cannot be seen in the marine cases because of a processing artifact: LWC can only be calculated when the droplet concentration is larger than 20 cm^{-3} , for statistical significance. Hence, for 25 June ($N_{ad} = 70 \text{ cm}^{-3}$) and 26 ($N_{ad} = 55 \text{ cm}^{-3}$), samples with a droplet concentration lower than $0.3N_{ad}$ and $0.4N_{ad}$ respectively, are not reported in the graph.

It must be noted that these 2 features do not appear similarly in the 8 graphs. The concentration/size relationship in quasi-adiabatic samples is more pronounced at low values of the mean droplet concentration, while the inhomogeneous mixing feature is more apparent at high mean concentration values. It is not clear yet if this difference reflects a physical phenomenon or the processing artifact mentioned above.

5. Effective diameter

As discussed in the scientific background section, cloud optical properties do not depend upon the mean volume diameter of the droplet size distribution but rather upon its effective diameter. However the adiabatic model and the above observations are applicable to the parameterization of the mean volume diameter. It is therefore necessary also to document relationships between d_v and $d_e = d_v^3/d_s^2$. For example, Pontikis and Hicks

(1992) and Martin et al. (1994) have shown that the coefficient $k = d_v^3/d_e^2$ varies from 0.67 ± 0.07 in continental air masses to 0.80 ± 0.07 in marine ones. Fig. 8 is a summary of the k distributions for the 8 flights of the CLOUDYCOLUMN campaign. The figure shows a scatter plot of the k values versus altitude above cloud base in the upper panel, and the k frequency distribution in the lower panel. Brenguier et al. (2000a) compare the radiative properties derived with a plane-parallel model (constant effective radius) and those derived with an adiabatic stratified model. They demonstrate that, for the derived reflectances in the visible and near infra-red to be equivalent in the 2 models, the value of effective radius in the plane-parallel model shall be between 5/6 and 100% of the value of effective radius at the top of the stratified model $r_e(H)$, depending on the values of H and N . $5/6r_e(H)$ is equivalent to $r_e(0.6H)$. The k frequency distributions are therefore restricted to the altitude range between $0.6H$ and H . The results confirm previous observations with the largest k values associated to marine air masses.

Since polluted clouds are characterized by smaller droplet sizes than the marine ones, this observation also suggests that k might be related to the droplet mean volume diameter. This statement is reinforced by the fact that in the k vertical profiles (Fig. 8), the values are lower at the cloud base, where droplets are smaller. In fact the feature reported by Pontikis and Hicks (1992) and Martin et al. (1994) is simply a consequence of the fact that the difference between the effective diameter and the mean volume diameter is limited to less than $3 \mu\text{m}$. Fig. 9 shows the difference as a function of d_v , for all the samples higher than $0.6H$ in the left panel, and the same samples after selection for adiabaticity and drizzle as in Fig. 4, in the right panel. The selection criteria reduce significantly the fraction of samples with a difference larger than $2 \mu\text{m}$. The variability is slightly lower in the polluted cases with smaller values of d_v (8 and 9 July). The flight on 16 July exhibits values up to 3. This flight shows also the broadest concentration distribution in Fig. 4 and the most scattered distribution of k in Fig. 8. The analysis of the

Fig. 9. Scatter plot of the $d_e - d_v$ versus d_v for samples above $0.6H$, for the same flights as in Fig. 4. Left panel: no selection. Right panel: with adiabaticity and drizzle selection as in Fig. 4.

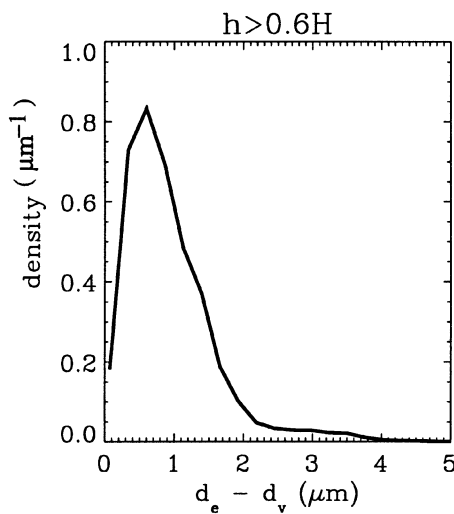


Fig. 10. Frequency distribution of $d_e - d_v$, for samples above $0.6H$, over the 8 flights shown in Fig. 9, without adiabaticity and drizzle selection.

aerosol properties below cloud base reveals that their distribution was not homogeneous in the boundary layer. Flight 16 is thus likely to correspond to uncommon aerosol properties and will need further analysis.

However, Fig. 10, for the $d_e - d_v$ frequency distribution calculated over the 8 flights, confirms that most of the $d_e - d_v$ values range between 0.2 and 1.8. The values of k reported previously are in agreement with this range. For example, a value 0.67 for continental clouds corresponds to $d_e - d_v = 1.5 \mu\text{m}$ with $d_v = 12 \mu\text{m}$ (see 8 July 1997 or 9 July 1997 in Fig. 9). Similarly, a value 0.80 for marine clouds corresponds to $d_e - d_v = 1.4 \mu\text{m}$ with $d_v = 20 \mu\text{m}$ (see 25 June 1997 or 26 June 1997 in Fig. 9). The parameterization of the cloud microphysical properties for radiative transfer calculations in stratocumulus clouds can be derived from the adiabatic model as follows. After the droplet concentration has been diagnosed from a parameterization of the activation process, the vertical profile of mean volume diameter is directly derived from the adiabatic LWC. The effective radius, required for the calculation of the local cloud radiative properties can then be approximated as $d_e = d_v + 1 \mu\text{m}$.

6. Conclusions

8 flights among the 11 performed during the CLOUDYCOLUMN campaign have been ana-

lyzed. Each flight is characterized by a typical value of droplet concentration. This value is derived as the mean of the frequency distribution of the values of droplet concentration measured at 10 Hz (10 m spatial resolution) during ascents and descents through the cloud layer. A selection procedure is applied to reject values affected by instrumental artifact, mixing effects and drizzle scavenging. The resulting distributions of concentration normalized by the mean value are similar for the 8 flights, ranging from 0.5 to 1.5 of the mean, and the mean value is dependent upon aerosol and CCN properties.

The frequency distributions of mean volume diameter versus altitude above cloud base reveal that droplets are growing according to the adiabatic model, with a variability corresponding to the variability in droplet concentration. The analysis of the correlation between concentration and size suggests that the variability of the droplet concentration in quasi-adiabatic regions is due to fluctuations of the updraft speed at cloud base, and that the decrease of LWC in sub-adiabatic regions is mainly due to a reduction of the droplet concentration, while droplet sizes are less affected by the mixing process (inhomogeneous mixing).

Finally, the relationship between the mean volume diameter and the effective diameter is examined. The CLOUDYCOLUMN data support previous conclusions from the ASTEX experiment, that the ratio $k = d_v^3/d_e^3$, increases from 0.67 in continental clouds to 0.80 in marine ones. In fact, it appears that such a feature can be simply explained by the fact that the difference between the effective and the mean volume diameters is almost constant at all altitudes above cloud base and in all types of clouds. The values of $d_e - d_v$ range between 0.2 and 1.8. Since the mean volume diameter increases with the altitude above cloud base, the ratio $k = d_v^3/d_e^3$ increases too and tends towards unity. For the same reason, namely that the mean volume diameter is larger in marine clouds than in the continental ones, at the same altitude above cloud base, the k -ratio is larger in marine clouds than in the continental ones.

A large sample of vertical profiles of the microphysics through stratocumulus clouds has been analyzed. It provides a firm validation of the adiabatic model for the parameterization of these profiles. With such a model it is possible to predict the LWC as a function of altitude and the droplet

effective diameter, when the droplet concentration is fixed. Integrals of the optical properties of the droplet spectrum over the cloud depth can then be derived. Further analysis is thus needed for the development of a parameterization of the droplet concentration as a function of the aerosol properties. Adiabatic cells cover only a fraction of a cloud system. The analysis presented here shows that the reduction of LWC in sub-adiabatic regions is mainly due to a reduction in droplet concentration, while the effective diameter is less altered by the mixing process. Therefore additional work is also needed for characterizing the effect

of sub-adiabatic regions on the radiative properties of a cloud system (inhomogeneous cloud bias).

7. Acknowledgements

The authors acknowledge the contributions of the ACE-2 participants, and particularly the METEO-FRANCE aircraft team for conducting Merlin-IV flights. This work has been supported by Météo-France, INSU, and the European Union under grant ENV4-CT95-0117.

REFERENCES

- Baker, M. B., Corbin, R. G. and Latham, J. 1980. The influence of entrainment on the evolution of cloud-droplet spectra (I). A model of inhomogeneous mixing. *Quart. J. Roy. Meteor. Soc.* **106**, 581–598.
- Barker, H. W. 1996. Estimating cloud field albedo using one-dimensional series of optical depth. *J. Atmos. Sci.* **53**, 2826–2837.
- Brenguier, J. L. 1991. Parameterization of the condensation process: a theoretical approach. *J. Atmos. Sci.* **48**, 264–282.
- Brenguier, J. L., Bourrianne, T., Coelho, A. A., Isbert, J., Peytavi, R., Trevarin, D. and Wechsler, P. 1998. Improvements of the droplet size distribution measurements with the Fast-FSSP. *J. Atmos. Oceanic Technol.* **15**, 1077–1090.
- Brenguier, J. L., Pawlowska, H., Schüller, L., Preusker, R., Fischer, J. and Fouquart, Y. 2000a. Radiative properties of boundary layer clouds: optical thickness and effective radius versus geometrical thickness and droplet concentration. *J. Atmos. Sci.*, in press.
- Brenguier, J. L., Chuang, P. Y., Fouquart, Y., Johnson, D. W., Parol, F., Pawlowska, H., Pelon, J., Schüller, L., Schröder, F. and Snider, J. 2000b. An overview of the ACE-2 CLOUDYCOLUMN closure experiment. *Tellus* **52B**, 815–827.
- Cahalan, R. F., Silberstein, D. and Snider, J. B. 1995. Liquid water path and plane-parallel albedo bias during ASTEX. *J. Atmos. Sci.* **52**, 3002–3012.
- Hansen, J. E. and Travis, L. D. 1974. Light scattering in planetary atmospheres. *Space Sci. Rev.* **16**, 527–610.
- Johnson, D. W., Osborne, S., Wood, R., Suhre, K., Johnson, R., Businger, S., Quinn, P. K., Wiedensohler, A., Durkee, P. A., Russel, L. M., Andreae, M. O., O'Dowd, C., Noone, K., Bandy, B., Rudolph, J. and Rapsomanikis, S. 2000. An overview of the Lagrangian experiments undertaken during the north Atlantic regional aerosol characterization experiment (ACE-2). *Tellus* **52B**, 290–320.
- Korolev, A. V. 1995. The influence of supersaturation fluctuations on droplet size spectra formation. *J. Atmos. Sci.* **52**, 3620–3634.
- Martin, G. M., Johnson, D. W. and Spice, A. 1994. The measurement and parameterization of effective radius of droplets in warm stratocumulus clouds. *J. Atmos. Sci.* **51**, 1823–1842.
- Pontikis, C. A. and Hicks, E. 1992. Contribution to the cloud droplet effective radius parameterization. *Geophys. Res. Lett.* **19**, 2227–2230.
- Russell, P. B. and Heintzenberg, J. 2000. An overview of the ACE-2 Clear Sky Column Closure Experiment (CLEARCOLUMN). *Tellus* **52B**, 463–483.
- Slingo, A. 1989. A GCM parameterization for the shortwave radiative properties of water clouds. *J. Atmos. Sci.* **46**, 1419–1427.
- Slingo, A. and Schrecker, H. M. 1982. On the shortwave radiative properties of stratiform water clouds. *Quart. J. Roy. Meteor. Soc.* **108**, 407–426.
- Snider, J. S. and Brenguier, J. L. 2000. A comparison of cloud condensation nuclei and cloud droplet measurements obtained during ACE-2. *Tellus* **52B**, 828–842.
- Twomey, S. and Cocks, T. 1989. Remote sensing of cloud parameters from spectral reflectance measurements in the near-infrared. *Beitr. Phys. Atmos.* **62**, 172–179.